Biophysical Chemistry 9 (1979) 329–344

SCANNING MOLECULAR SIEVE CHROMATOGRAPHY OF INTERACTING PROTEIN SYSTEMS IV. THE DIFFERENCE PROFILE METHOD AS APPLIED TO THE GIBBS-DUHEM EXPRESSION IN THE ANALYSIS OF THE DIMER-TETRAMER EQUILIBRIA OF OXYHEMOGLOBIN A*

Eugene E. SAFFEN, Jr. and Paul W. CHUN *
Department of Biochemistry and Molecular Biology, College of Medicine, University of Florida, Gainesville, Florida 32610, USA

Received 19 September 1978

The recently-developed large zone difference profile method in scanning molecular sieve chromatography is applied to the analysis of the Gibbs-Duhem expression in the tetramer–dimer equilibrium of human oxyhemoglobin A. The preferential binding term and solvation parameters of the Hofmeister anion phosphate are examined. Results indicate that as the concentration of phosphate ions increase, a hydrated phosphate is formed which enhances the association by perturbing the solvation layer of the hemoglobin molecules. The standard free energy change at a given Hofmeister anion activity of $\ln A_X = -3.2476$ is 9.4 ± 0.2 kcal/mole. ΔG^0 at $\ln A_X = -1.2711$ is 10.90 ± 0.05 kcal/mole, suggesting that approximately 11 kcal are required to dissociate one mole of tetramer into dimer.

1. Introduction

The recent introduction of direct ultraviolet scanning of a gel column [1,2] has greatly advanced previous elution techniques by permitting direct analysis of solute profiles at many stages during a single column experiment. Large zone or saturation experiments [2] afford the most accurate determination of the solute partition cross-section (ξ_i) and the partition coefficient (σ_i).

The recently-developed difference profile method [3,4] permits analysis of the time-dependent properties of large-zone solute profiles at concentrations as low as 2 μg/ml.

Measurement of the dissociation of hemoglobin into its αβ dimer at neutral pH and low ionic strength (at concentrations as low as 10 μg/ml) has been studied by analytical molecular sieve chromatography [5,6] in order to ascertain the dimer–tetramer stoichiometry for oxyhemoglobin and to provide information about free energy of interaction of the subunits under these experimental conditions [7–9]. The equilibrium constants for dimer–tetramer association of oxyhemoglobin as a function of temperature have been extensively examined by molecular sieve chromatography and calorimetric measurements [10–12]. to assess the structural and energetic changes which accompany oxygenation. Barksdale and Rosenberg [13] have used the tritium–hydrogen exchange procedure to study the temperature, pH and anion dependence of the carboxyhemoglobin A dimer–tetramer equilibrium. The free energy coupling between oxy and deoxyhemoglobin for tetramer–dimer dissociation has been reported to be on the order of 6 or 8 kcal [10,14,15]. This intersubunit bond appears to be the strongest of bonding interactions within the hemoglobin tetramer [11,12,16,17] and undergoes large structural changes upon oxygenation [18–20].

The effect of sodium chloride on the association of hemoglobin subunits has been analyzed by procedures based primarily on the dimer molecular weight expressed as a buoyancy term, $M_2\ (\partial\rho/\partial C_2)$. Here the variation of the reduced intensity increment as a function of the solvent density, ρ_0, reflects both the

* This work was supported by NSF PCM 76-04367 and in part by University computer research support, College of Arts and Sciences, University of Florida.
* Address correspondence to P.W. Chun, Department of Biochemistry and Molecular Biology, College of Medicine, Box J-245, University of Florida, Gainesville, Florida 32610.

the changes in preferential interaction of a Hofmeister series of anions, where $(\partial\rho/\partial C_2) = (1 - \phi'\rho_0)$, as well as alterations in the partial specific volume [14,16,21].

In a paradoxical contrast to its accepted role as a dissociating agent (Hofmeister effect), sodium chloride has been reported to increase the degree of self-association of α^{sH} and β^{sH} hemoglobin chains [11, 22]. To date, however, no data is available on the application of the Gibbs-Duhem expression to determine the varied effects of a Hofmeister series of anions on the association–dissociation equilibria of oxyhemoglobin A.

In this communication, we describe the experimental determination of difference profiles for the tetramer–dimer equilibrium of oxyhemoglobin by scaning molecular sieve chromatography. Through application of the Gibbs-Duhem expression, we attempt to define alterations in the isothermal equilibrium conditions when the associating system is perturbed by the phosphate anion, one of a Hofmeister series of anions [23];

2. Experimental procedures

2.1. Materials and methods

All gel chromatography experiments were performed on Sephadex G-100 regular, obtained from Pharmacia. Marker proteins such as cytochrome C, chymotrypsin (3X), sperm whale myoglobin, ovalbumin (5X) and bovine serum albumin were purchased commercially from Schwarz-Mann (Orangeberg, NY). Glycylglycine and Trisma were obtained from Sigma Chemical Co., St. Louis, MO. Hemoglobin samples were prepared from freshly drawn blood by the method of Williams and Tsay [24] and all experiments for each sample of normal human hemoglobin were performed within two days. Concentration of the hemoglobin (HbA) in solution was determined by extinction coefficients of $E_{mM}^{280\,nm} = 34.0$ and $E_{mM}^{577\,nm}/E_{mM}^{547\,nm} = 1.066$. Given molal concentrations of NaH_2PO_4 and Na_2HPO_4 are adjusted to pH 7.4 giving a total phosphate concentration of 0.05 M, with an ionic strength of 0.1. A solution of 0.5 M phosphate, (μ = 1.0) would crystallize below 4°C, therefore all experiments were run at 25°C.

2.2. Scanning chromatograph with Nova Z/4 data acquisition system

The scanning system used in these experiments is essentially the same as that described elsewhere [1,2]. with the exception of the monochromator and lamp housing, which are GM250 spectrophotometer model EU-700 (grating monochromator) and EU-701-50 (light source module) housing a Beckman deuterium lamp. All experimental data were obtained at 2200 Å with a single 2240 Å (±202 Å, half-width) band pass optical filter (Baird-Atomic 35-02-0, 25 mm diameter) inserted between the monochromator and column compartment.

The data acquisition and processing system consists of Nova Z/4 mini-computer (Data General Corp., 16K, 16-bit words of core memory) and a multi-purpose interface unit (Olis Model No. 3600) developed by On-line Instrument Systems [3]. Commands to the interface program are entered via an ASR33 teletype. Data may be output to a storage oscilloscope (Tektronix D11), to an $X - Y$ plotter (Hewlett-Packard 7005-B) and to punch tape and/or printed hard copy via the teletype. For data storage and manipulation, we use the computer facilities of the Northeast Regional Data Center, University of Florida. Operation of the system has been extensively described elsewhere [25,26].

2.3. Column packing

The quartz column (25 cm × 0.975 cm) was packed under gravity with Sephadex G-100 regular, previously swollen in Na-phosphate buffer of varying concentrations at pH 7.4.

Glass wool served as the base on which the gel bed was packed. A porous polyethylene disc was used to stabilize the top of the gel column and an LKB varioperpex pump was used to maintain a constant flow rate of approximately 4.01 ml per hour. For these experiments, a single column was used throughout and the area was 0.567 cm^2 (radius, 0.425 cm).

The activity coefficients of NaH_2PO_4 were calculated from the curve shown in fig. 1, derived from eq. (12), based on the data of Robinson and Stokes [27], and compared with the CRC Handbook of Chemistry and Physics [28].

2.4. Large zone profile transport experiments

Data on column partitioning were obtained exclusively by the use of large zone transport experiments. The gel column was equilibrated with phosphate buffer of varying concentrations at pH 7.4. In this type of experiment, a hemoglobin solution at the desired concentration was added continuously to the column, which is scanned repeatedly at regular intervals until a reproducible baseline is obtained. The criterion for reproducibility of such large zone scans was established to be that the mean difference in absorbance at each point in the column between two consecutive scans not exceed 0.001 absorbance units. The column is scanned at regular time intervals as the solution/solvent boundary moves through the gel matrix at a constant flow rate of 4.0 ml/hour.

In the difference profile method of analyzing such large zone experiments, 300-point unit records of successive scans are subtracted from each other, matrix-wise, yielding difference profiles. The problem of locating the centroid position of each boundary is then reduced to the simple problem of locating the peak position of these difference profiles. For a 300-point profile, location of the peak position to within ±3 points results in a position error of ±1%. This procedure has proved itself in yielding exceptionally accurate $(dt/d\bar{x})$ values. Partitioning calibration parameters for a given column are obtained by determining the rate of movement of a series of sample macromolecules of known molecular radius [29,30]. The partition coefficient is calculated from

$$\sigma = \frac{(dt/d\bar{x})_P - (dt/d\bar{x})_0}{(dt/d\bar{x})_I - (dt/d\bar{x})_0} \tag{1}$$

where $(dt/d\bar{x})_P$ is the slope of a plot of t versus $\bar{x}$ for a given sample marker, $(dt/d\bar{x})_0$ is the slope of the void volume marker and $(dt/d\bar{x})_I$, the slope of the internal volume marker. The values of $(dt/d\bar{x})_P$ for the hemoglobin sample correspond to $(1/F)\,dV/d\bar{x}$, where F is the flow rate and $(dV/d\bar{x}) = (\alpha + \beta\sigma)$, in which the slope of the plot of volume versus peak position, $\bar{x}$, is used to calculate the partition coefficient σ. α is the void volume per unit column length and cross-sectional area and β is the internal volume fraction of the gel phase per unit column length and cross-sectional area, i.e. $\xi = (\alpha + \beta\sigma)$. Note that the values of $\bar{x}$ were taken directly as the point numbers corresponding to difference profile peaks. Values of t, time, were calculated as the average between the times at which the two scans used to obtain the difference profile were taken, i.e. $t_{(x)} = t_{i-1} + [(t_i - t_{i-1})/2]$. The partition cross-section, ξ, is calculated from the following fundamental expression [30,31]

$$\xi A = F(dt/d\bar{x}). \tag{2}$$

The partition cross-section, ξ, represents the fraction of column cross-sectional area, A, which is accessible to the solute. This quantity ξ is dependent on the position of x within the gel bed. The expression for the weight average partition cross-section of interacting solute, which we denote as $\bar{\xi}_w$ is:

$$\bar{\xi}_w = \sum_i (\xi_i C_i/C) + \beta_1' C + \beta_2' C^2. \tag{3a}$$

The expression for the weight average partition coefficient is:

$$\bar{\sigma}_w = \sum_i (\sigma_i C_i) + \beta_1 C + \beta_2 C^2, \tag{3b}$$

where $C = \Sigma_i C_i = \Sigma_i K_i C_1^i$. For a given concentration C_i, the following expression is used, where erfc is the error function complement [29], in order to relate the partition coefficient σ_i to the molecular radius a_i.

$$a_i = a_0 + b_0 \operatorname{erfc} \sigma_i. \tag{4}$$

Here a_0 and b_0 are calibration constants of a particle of given radius in a given gel and are determined independently.

2.5. Evaluation of centroid positions ($\bar{x}$) of trailing and leading boundaries by the difference profile method

In cases where determination of the difference profiles of leading and trailing boundaries requires numerical approximation of the delta function in terms of the time reference frame, i.e. $F_{(t,x)}$, this function may be expressed as [30,31]

$$F_{(t,x)} = \frac{C_0}{\sqrt{4\pi LVt}} \exp\left\{-\frac{[x - (V/\xi)t]^2}{4LVt}\right\}. \tag{5}$$

Letting C_0 represent the plateau concentration, $a = 4LV$, where L is the axial dispersion coefficient and V is the solute distribution volume of the leading and trailing edges of the boundary. The centroid position, $\bar{x} = V/\xi$ and $C' = C_0/\sqrt{4\pi LV}$.

(i) The centroid position of the trailing boundary $\bar{x}$, after difference profile determination, may be directly evaluated from

$$F_{(t+\Delta t,x)} - F_{(t,x)}$$

$$= C'\Delta t \int_{-\infty}^{x} \frac{\mathrm{d}}{\mathrm{d}t}\frac{1}{\sqrt{t}} \exp[-(x-\bar{x}t)^2/at]\,\mathrm{d}x. \qquad (6)$$

Assuming the time interval between scans, Δt, is limited to 5 ~ 10 minutes, then eq. (6) yields

$$F_{(t+\Delta t,x)} - F_{(t,x)}$$

$$\approx \frac{C'\Delta t}{t^2}\{\bar{x}\exp[-(x-\bar{x}t)^2/at]\}, \qquad (7)$$

providing that $\xi_{(x)}$ remains constant within this time interval and noting that $\xi_{(x)}$ varies with the distance coordinate in self-associating systems.

(ii) The centroid positions of the leading boundary may be determined from the same equation, noting that the distribution curve is quite distinct from that of the trailing boundary. At the centroid position, $\bar{x}$, the distribution function is expressed as

$$F_{(t+\Delta t,x)} - F_{(t,x)}$$

$$\approx \frac{C_0\bar{x}\Delta t}{\sqrt{4\pi LVt^2}} \exp[-(x-\bar{x})^2/4LVt]. \qquad (8)$$

Eq. (8) may be used to locate the centroid positions of the transport boundaries for any associating system of the monomer–dimer type as a function of concentration, noting that the expression deals with the difference boundary profile, rather than the derivatives of the large zone profile.

2.6. Thermodynamic analysis of the Gibbs-Duhem expressions

The standard Gibbs free energy of association, as a function of the ion pair activity of the salt (A_x), activity of water (A_w) and temperature of 1 : 1 electrolytes, has been described [26]

$$\mathrm{d}\ln K_{eq} = (\partial \ln K/\partial \ln A_x)_{A_w,T}\,\mathrm{d}\ln A_x + (\partial \ln K/\partial \ln A_w)_{A_x,T}\,\mathrm{d}\ln A_w + (\partial \ln K/\partial T)_{A_x,A_w}\,\mathrm{d}T, \qquad (9)$$

where A_{H^+} and pressure (P) remain constant. Integration of eq. (9) yields

$$\ln K_{eq} = [\Delta\bar{\nu}_x - (n_x/n_w)\Delta\bar{\nu}_w]\ln A_x + \int_{T_i}^{T_f} (\partial \ln K/\partial T)\mathrm{d}T, \qquad (10)$$

where

$$(\partial \ln K/\partial \ln A_x) = \Delta\bar{\nu}_x, \quad (\partial \ln K/\partial \ln A_w) = \Delta\bar{\nu}_w$$

and

$$\mathrm{d}\ln A_w = -(n_x/n_w)\mathrm{d}\ln A_x.$$

Based on eq. (10), at a constant temperature

$$\ln K_{eq} = \Delta\bar{\nu}_w \ln A_x + \Delta\bar{\nu}_w \ln A_w + C, \qquad (11)$$

where

$$C = \int_{T_i}^{T_f} (\partial \ln K/\partial T)\mathrm{d}T\ .$$

C remains constant where $\mathrm{d}T = 0$. T_i is the initial temperature of the experiment and T_f is the final temperature.

The values of $\ln A_x$ are extracted from Robinson and Stokes [27] and compared with the CRC Handbook of Chemistry and Physics [28], noting that $\ln A_w$ is calculated from $-(n_x/55.56)\ln A_x$. Linear regression analysis is used to determine the coefficients of $\ln A_x$ and $\ln A_w$ where $\ln K_{eq}$ is a function of $\ln A_x$ at a given temperature.

2.7. Methods of computation

All calculations in the computation of the Gibbs-Duhem equation [11] and the molecular sieve partition equation (3) were done using general linear models (SAS GLM procedure, Barr et al. [32]), which use the principle of least squares to fit a fixed-effect linear model to virtually any type of univariate and multivariate analysis, including simple linear re-

gression, multiple linear regression, analysis of variance, analysis of covariance, and partial correlation analysis.

The statistical analysis system language, interfaced with PL/1, was utilized for all routines (GLM 127, GLM 131).

The stepwise regression procedure (STE 251, Barr et al. [32]) which was applied to our analysis of thermodynamic parameters includes five techniques to find the variable of a collection of independent variables which is most likely to be included in a regression model. This method of computation was extremely useful for data screening, permitting some insight into the relative strengths of the relationship between proposed independent variables and dependent variables (largest R^2 statistic). The five-part procedure includes: 1) a forward selection technique which finds first the single-variable model, 2) a backward elimination technique which is first performed for a model including all the independent variables, 3) stepwise modification of the forward selection, 4) and the maximum R^2 improvement and 5) minimum R^2 improvement. The fourth and fifth procedures produce models which fit the data equally well in our computation.

3. Results

The activity coefficient of the total phosphate in a series of buffer solutions of NaH_2PO_4, pH 7.4, as a function of molal concentration was extracted from the CRC Handbook of Chemistry and Physics [28], as shown in fig. 1. The solid line represents the theoret-

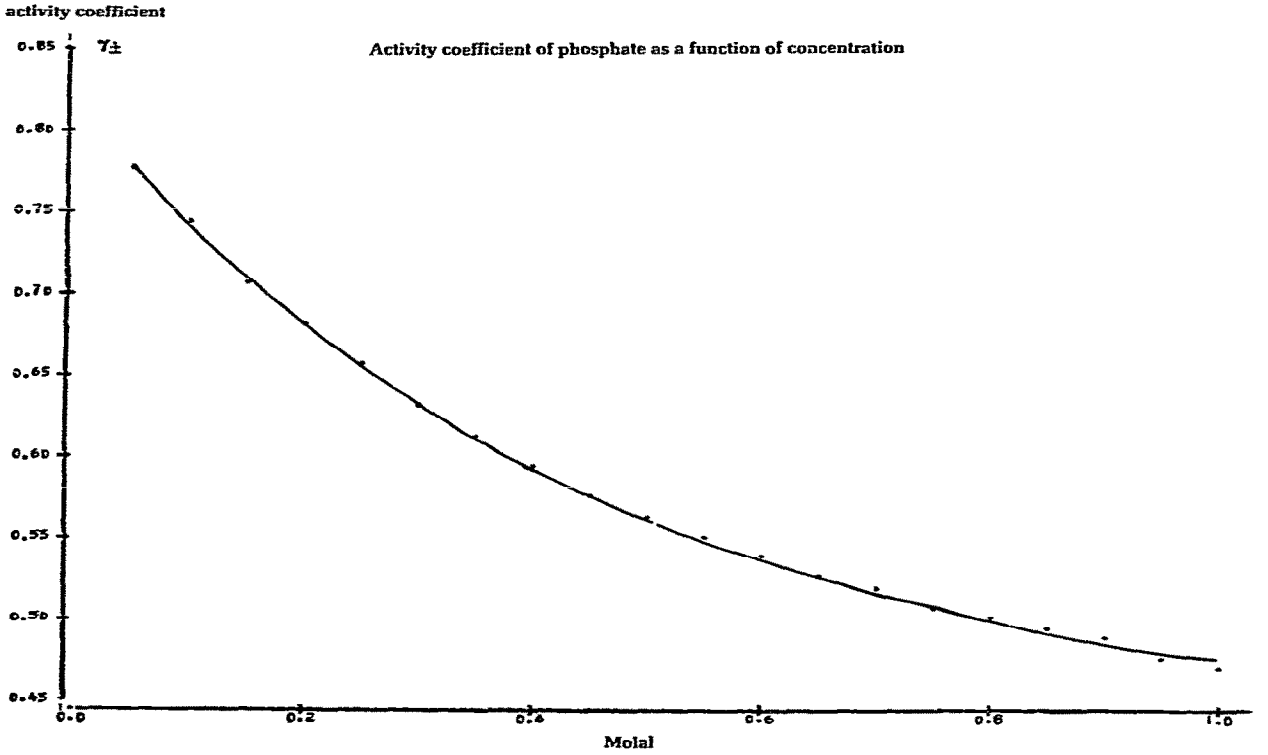

Fig. 1. Activity coefficient as a function of the total phosphate concentration. Data were extracted from the CRC Handbook of Chemistry and Physics [28] at 25°C. The curve was fitted to a general linear model by the expression: $\gamma_{\pm PO_4^{-3}} = \alpha + \beta C + \gamma C^2 + \delta C^3$.

ical data, which is best fitted to a general linear model by the following expression:

$$\gamma_{\pm PO_4^{-3}} = [\alpha + \beta C^2 + \gamma C^2 + \delta C^3] \quad (12)$$

where $\alpha = 0.8173$, $\beta = 0.8403$, $\gamma = 0.8216$, and $\delta = -0.3317$ with a standard deviation of 0.0028. The values of the residue square (R^2) and F-test show that the data of $\gamma_{\pm}$ versus molal concentration fit the theoretical curve within a 99.9% confidence limit ($PR > F = 0.0001$). All values of the activity of the buffer system at a given pH were determined based on fig. 1. The ionic strength of phosphate buffers used in these experiments varied from 0.1 to 1.0.

In figs. 2A, B, C, showing the trailing boundary of the difference profiles, the location of the cursor indicates the centroid position of the hemoglobin sample in 0.05 M phosphate as it moves down the column into 0.05 M phosphate and 2 M NaCl.

In these figures, the slower moving components, which appear as either a peak or a dip in the profile behind the centroid position, represent the difference in the index of refraction of the two solvent phases, 0.05 M phosphate and 0.05 M phosphate and 2 M NaCl. Thus, the slow-moving peak represents an interface between low and high ionic strength buffer solutions. Conversely, the interface between a high and low ionic strength buffer solution is marked by a dip, seen in figs. 2D, E, F.

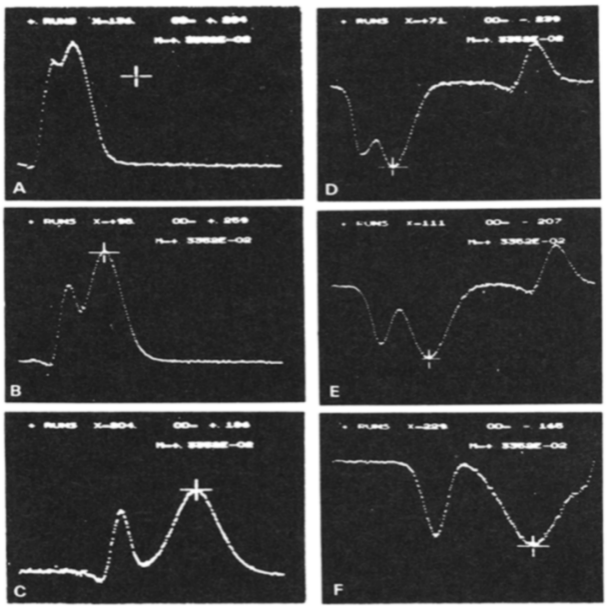

Fig. 2. Difference profiles of the leading (A, B and C) and trailing (D, E and F) boundaries for human oxyhemoglobin in high (A, B and C) and low (D, E and F) ionic strength phosphate buffer, pH 7.4, at the interface between 0.05 M phosphate and 0.05 M phosphate + 2 M NaCl.

These difference profiles reveal that the degree of solvent-solvent and solvent-solute interaction varies with the leading and trailing edge of the reaction boundary as a result of different solvent ionic strengths. Hence the large zone difference profiles between two solvent systems may be photographed at varying time intervals and used to locate the centroid position as a function of column length as the hemoglobin sample moves down the column.

The series of photographs in fig. 3 shows the difference profiles of scans taken 55 minutes after formation of the leading or trailing boundary. Figs. 5A–E show five samples at different hemoglobin concentrations in 0.05 M phosphate buffer; figs. 5F–J represent five additional samples in 0.1 M phosphate buffer, varying the hemoglobin concentration. Each scan represents 300 data points, which are converted to absorbance values using a reference intensity determined while the column is out of the light beam just prior to each run.

Figs. 4a and 4b show representative original data profiles based on a plot of the centroid position ($\bar{x}$) of the difference profile as a function of time for various concentrations of hemoglobin solutions. The correlation of the partition cross-section (ξ_w) and the partition coefficient (σ_w) as a function of $dt/d\bar{x}$ (min/pts) was found to be 0.9999 at all concentrations.

Values for the partition coefficient as a function of concentration in varying phosphate buffers, pH 7.4, are shown in fig. 5 and table 5. In analyzing the effect of phosphate anions on the tetramer–dimer equilibrium of oxyhemoglobin, we find that the degree of dissociation of $\alpha_2\beta_2$ into $\alpha\beta$ dimer is influenced by the total concentration of phosphate anions.

We have previously reported the partition coefficient and partition cross-section for the $\alpha\beta$ dimer in 0.05 M phosphate + 2 M NaCl, pH 7.4, as 0.365 ± 0.005 and 0.419 ± 0.002, respectively [3]. Table 1 and fig. 5 (curve #1) demonstrate the values of the partition cross-section and partition coefficient in 0.05 M phosphate, pH 7.4, over the solute concentration range 100–10 μg/ml.

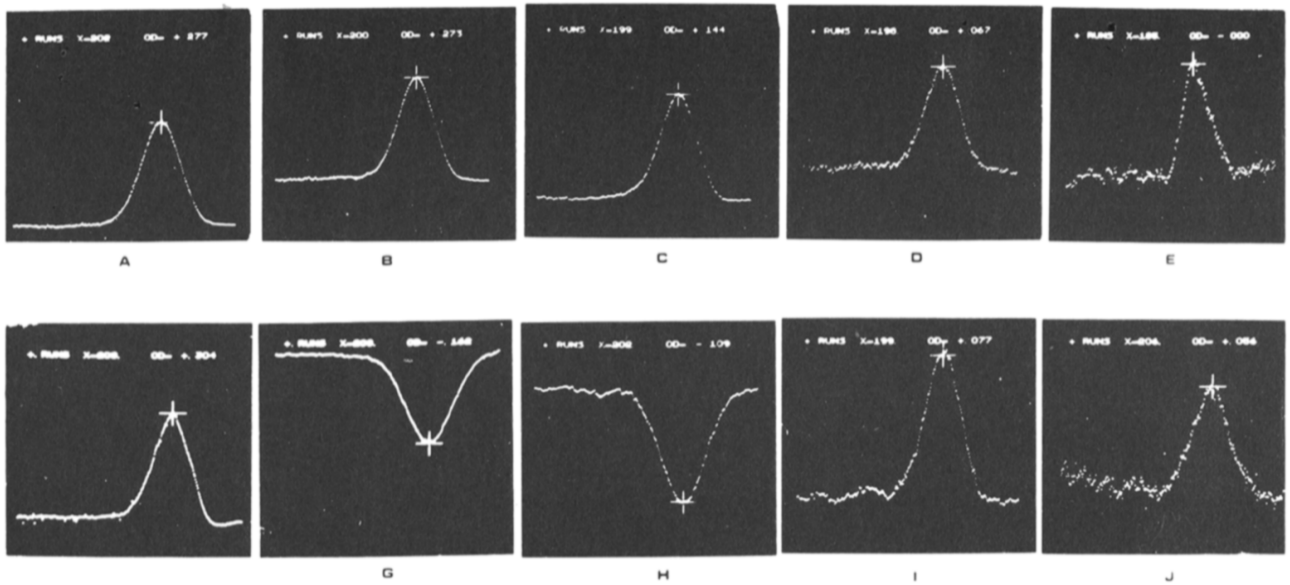

Fig. 3. Difference profiles of the leading (A, B, C, D, E, F, I and J) and trailing boundaries (G and H) at varying concentrations of oxyhemoglobin. All profiles are the difference between scans recorded at 45 minutes and 55 minutes after formation of large zone boundary. Figures A, B, C, D, and E are in 0.1 M phosphate buffer and F, G, H, I, and J are in 0.05 M phosphate at pH 7.4.

A) $-0.05 \leqslant$ O.D $\leqslant +0.55$, 100 μg/ml
B) $-1.0 \leqslant$ O.D $\leqslant +0.40$, 75 μg/ml
C) $-0.05 \leqslant$ O.D $\leqslant +0.25$, 50 μg/ml
D) $-0.05 \leqslant$ O.D $\leqslant +0.10$, 25 μg/ml
E) $-0.05 \leqslant$ O.D $\leqslant +0.10$, 10 μg/ml
F) $-0.10 \leqslant$ O.D $\leqslant +0.50$, 100 μg/ml
G) $-0.35 \leqslant$ O.D $\leqslant +0.05$, 75 μg/ml
H) $-0.15 \leqslant$ O.D $\leqslant +0.05$, 50 μg/ml
I) $-0.01 \leqslant$ O.D $\leqslant +0.09$, 25 μg/ml
J) $-0.02 \leqslant$ O.D $\leqslant +0.07$, 10 μg/ml

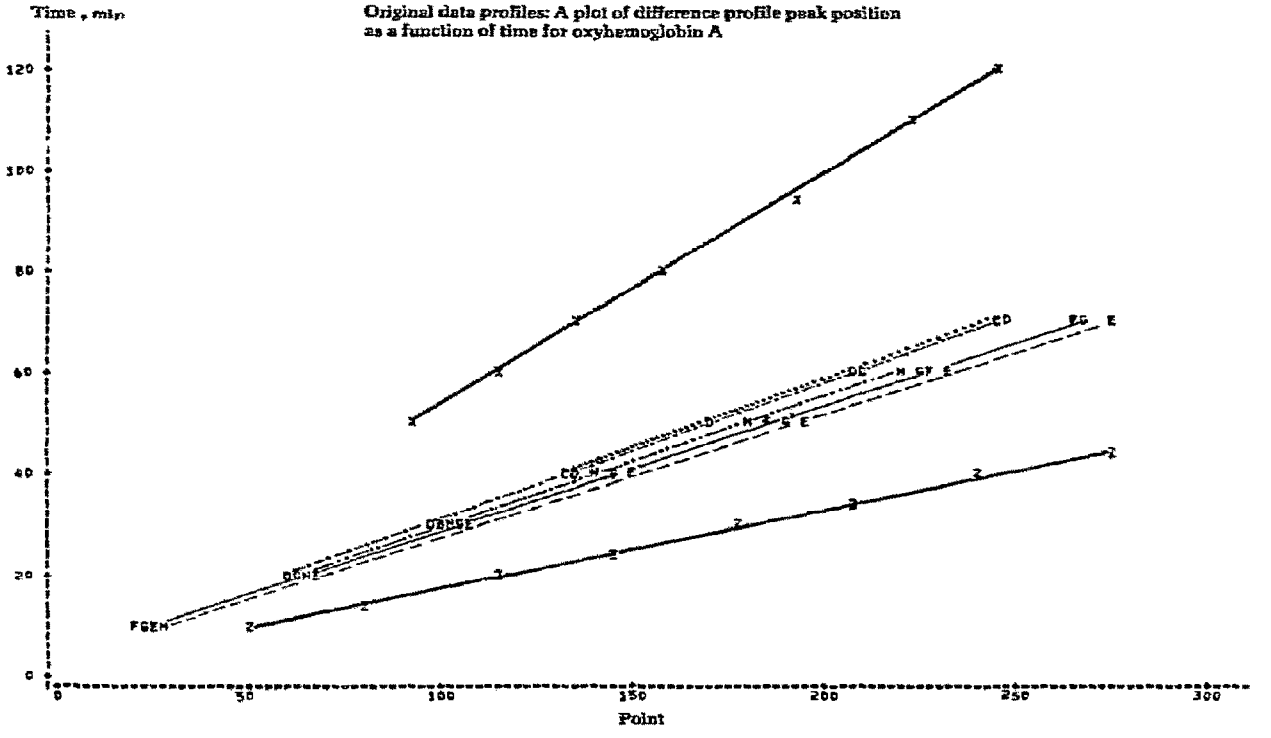
Time , min
Original data profiles: A plot of difference profile peak position as a function of time for oxyhemoglobin A
120
100
80
60
40
20
0
0
50
100
150
200
250
300
Point

Fig. 4a

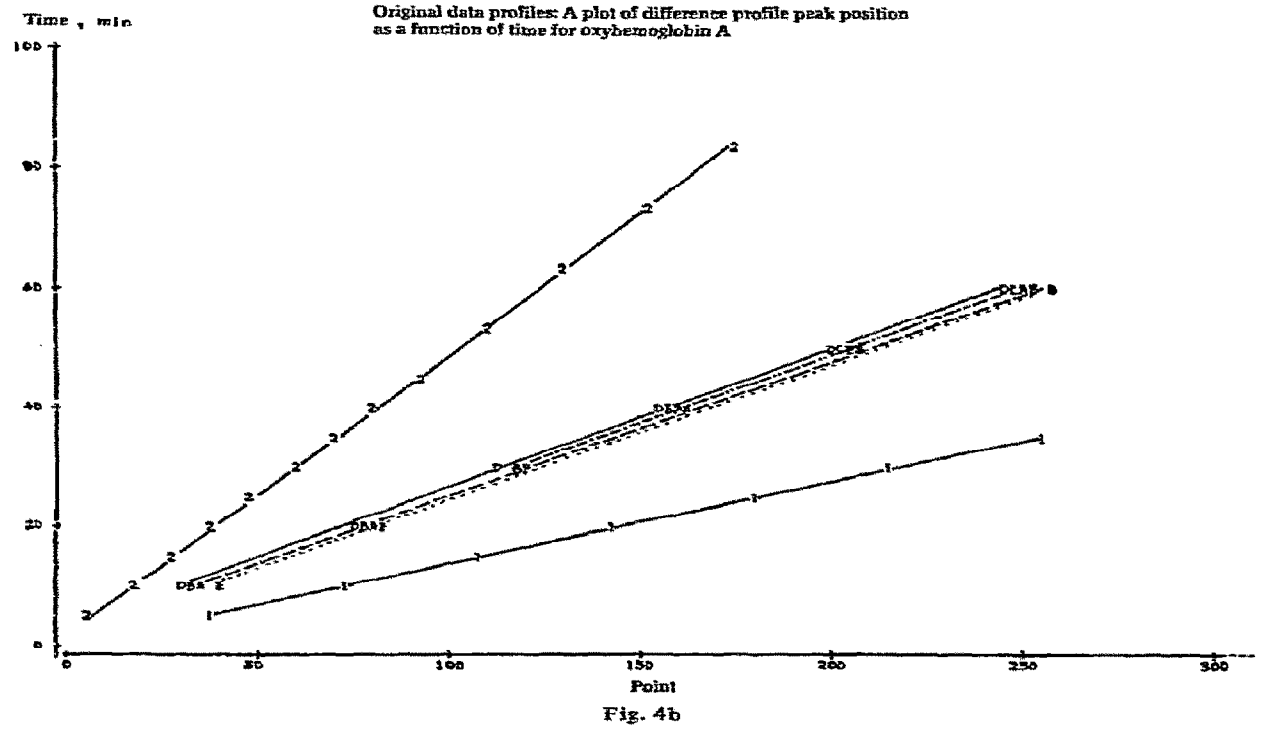
Time , min
Original data profiles: A plot of difference profile peak position as a function of time for oxyhemoglobin A
100
80
60
40
20
0
0
50
100
150
200
250
300
Point

Fig. 4b

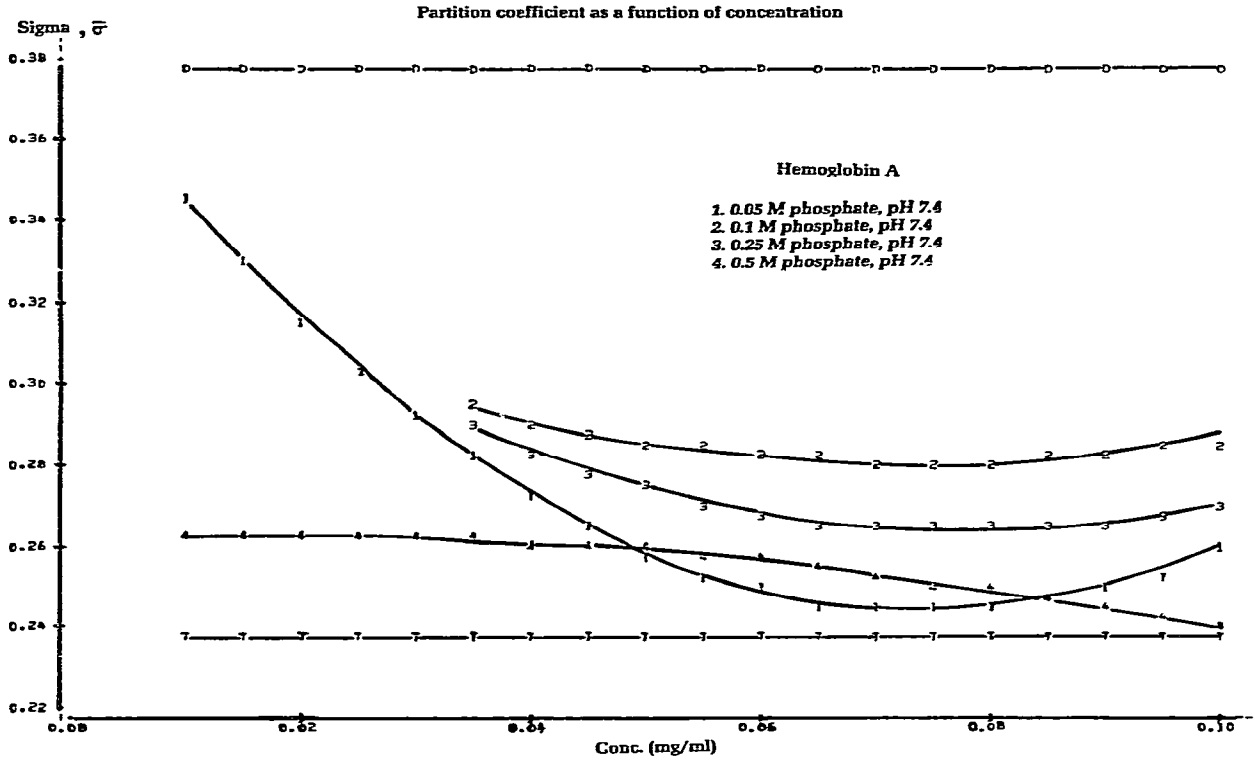

Fig. 5. Partition coefficients of oxyhemoglobin A as a function of concentration in phosphate buffers of varying concentration. Horizontal lines designated D and T represent dimer and tetramer respectively.

Our experimental data points were fitted to eq. (3) to generate the curves of fig. 5, where $f_1 = (\bar{\sigma}_w - \sigma_2)/(\sigma_1 - \sigma_2)$, based on a dimer–tetramer model for oxyhemoglobin association, as shown in table 5. The equilibrium constants were calculated based on

$$K_2 = (\bar{\sigma}_w - \sigma_1 f_1 - \beta_1 C - \beta_2 C^2)/(\sigma_2 f_1{}^2 C) \qquad (13)$$

to regenerate $(\bar{\sigma}_w/C) = (\Sigma_i \sigma_i f_i)/C + \beta_1 + \beta_2 C$, insuring that the values of the virial coefficients β_1 and β_2 were consistent.

The variations in the partition radii (in Å) as a function of concentration in various phosphate buffers are shown in fig. 6, where each curve is generated by fitting data points to the expression: $a_i = a_0 + b_0$ erfc σ_i. Values for a_0 and b_0 of 8.9 Å and 23.4 Å, respectively, were determined based on the experimentally-

Fig. 4a. Original data profiles (time versus points) for oxyhemoglobin A at different concentrations. All profiles represent the difference between scans taken 5, 15, 25, 35, 45 and 55 minutes after formation of the large zone boundary. Number x is the inclusion marker, and z is the void volume marker. A, B, C, D are in 0.05 M phosphate +2 M NaCl. E, F, H and H are in 0.05 M phosphate buffer, pH 7.4. $\alpha = 0.327$, $\beta = 0.596$ and $\xi = (0.327 + 0.59\sigma)$. $\xi = (F/A)(dt/d\bar{x})$. Scanning rate = 0.1949 cm s^{-1}, scanning distance = 16.18 cm. Number of points/unit distance in the scanner = 18.545 pts cm^{-1}. A) 43 μg/ml, B) 32 μg/ml, C) 22 μg/ml, D) 9 μg/ml, E) 43 μg/ml, F) 32 μg/ml, G) 22 μg/ml, H) 9 μg/ml.

Fig. 4b. Original data profiles (time versus points) for oxyhemoglobin A at different concentrations. All profiles represent the difference between scans taken 5, 15, 25, 35, 45 and 55 minutes after formation of the large zone boundary in 0.1 M phosphate buffer, pH 7.4. A) 100 μg/ml, B) 75 μg/ml, C) 50 μg/ml, D) 25 μg/ml, E) 10 μg/ml.

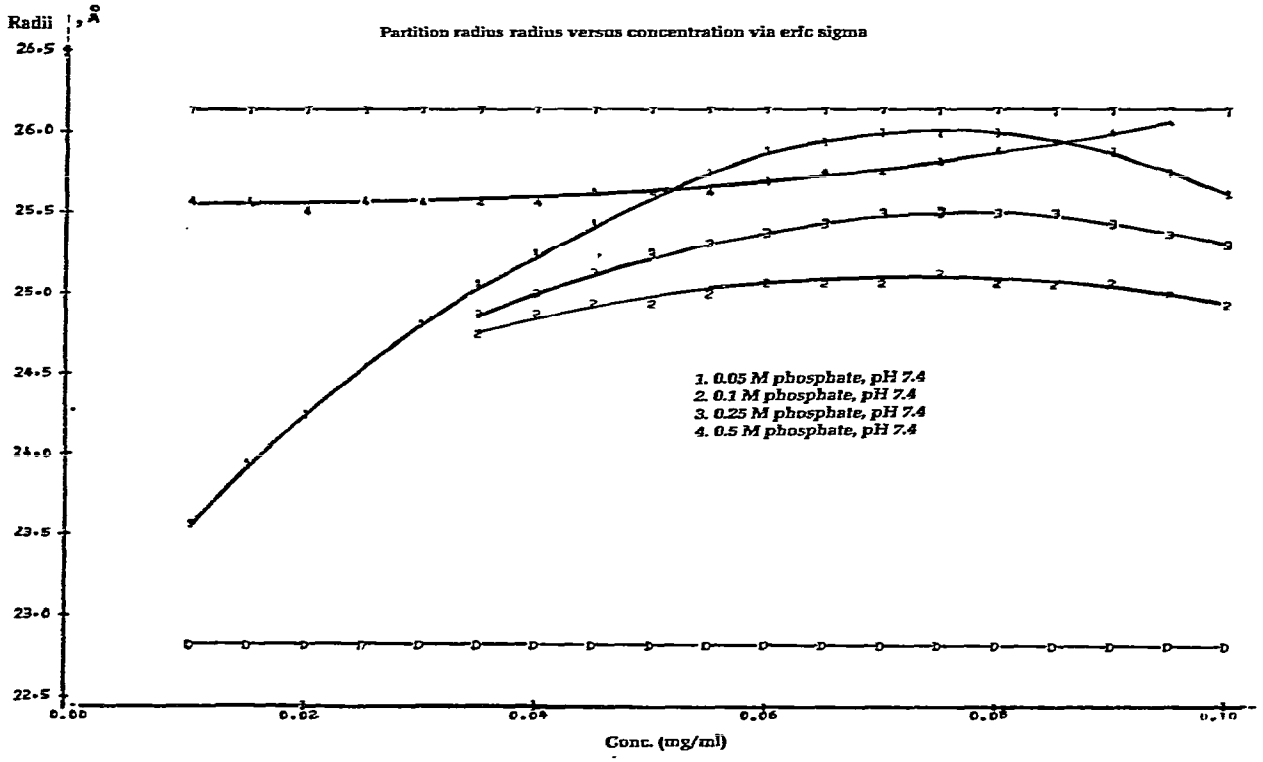

Fig. 6. Partition radii as a function of oxyhemoglobin concentration in different phosphate buffers. Partition radii were evaluated from $a_i = a_0 + b_0$ erfc σ_i. Horizontal lines designated D and T represent dimer and tetramer, respectively.

obtained molecular radius (Stokes) calibration constants of cytochrome C (18.0 Å, $\sigma = 0.606$), chrymotrypsin (22.5 Å, $\sigma = 0.403$) and ovalbumin (27.6 Å, $\sigma = 0.187$) [3]. The Stokes radii ($\mathring{r}$) were calculated from the following expression:

$$\mathring{r} = r_0(f/f_0)\{1 + (i - 1)f_2\}^{1/3} \qquad (14)$$

where r_0 is the partition radius of dimer 23.4 Å. The frictional ratio, f/f_0, is 1.104; i is an integer equal to the number of subunits in the i-mer; and f_2 is the weight fraction of the tetramer. The values for the dimer and tetramer were determined to be 25.4 Å and 31.9 Å, respectively. The variation between partition and Stokes radii as a function of concentration for varying phosphate buffers are shown in tables 1–5 and fig. 6.

A summary plot of the partition radii (Å) as a function of the erfc (σ) at various hemoglobin concentrations, shown in fig. 7, obeys a strictly linear relationship.

Fig. 8 shows a Gibbs-Duhem plot of ln Keq versus ln A_x, the phosphate ion activity, where the curves are regenerated representations of different hemoglobin concentrations undergoing tetramer–dimer dissociation as a function of phosphate concentration.

The effect on the solvation parameters ($\Delta\bar{\nu}_x$ and $\Delta\bar{\nu}_w$) are shown in table 6. Unfortunately, the curve fitting procedure used here makes it extremely difficult to precisely evaluate the two parameters. Some general conclusions, however, may be drawn from the data. The slopes of $(d\ln A/d\ln A_x) = \Delta\bar{\nu}_{pref}$ (from eq. 10) are all positive values, indicative of a salting-out phenomenon with increasing phosphate concentration which would favor association. $\Delta\bar{\nu}_{pref}$ values are all negative, and $\Delta\bar{\nu}_w$ positive, over the concentration range examined.

Table 1
Molecular sieve parameters and free energies for the dimer–tetramer equilibrium of oxyhemoglobin in 0.05 M phosphate buffer, pH 7.4, at 25°C

Conc (μg/ml)	ξ_i	σ_i	erfc σ_i	$\mathring{A}$	$\mathring{r}$	f_1	ln K	ΔG^0 (kcal/mole)
100	0.5149	0.2592	0.7140	25.6	30.8	0.151	15.09	−8.95
85	0.5058	0.2464	0.7275	26.0	31.3	0.061	16.68	−9.88
75	0.5040	0.2439	0.7201	26.9	31.4	0.042	17.21	−10.19
50	0.5146	0.2587	0.7145	25.9	30.8	0.148	10.29	−9.65
45	0.5193	0.2653	0.7076	25.5	30.6	0.195	15.64	−9.46
35	0.5313	0.2819	0.6901	25.1	29.9	0.314	15.33	−9.08
25	0.5467	0.3035	0.6678	24.5	28.9	0.468	14.76	−8.75
10	0.5762	0.3447	0.6259	23.6	26.9	0.762	14.02	−8.31

ln A_X = −3.2476 and ln A_W = 0.00293. $\mathring{r}$ is the Stokes radius and $\mathring{A}$ is partition radius (in A units).

Table 2
Molecular sieve parameters and free energies for the dimer–tetramer equilibrium of oxyhemoglobin A in 0.1 M phosphate buffer, pH 7.4, at 25°C

Conc (μg/ml)	ξ_i	σ_i	erfc σ_i	$\mathring{A}$	$\mathring{r}$	f_1	ln K	ΔG^0 (kcal/mole)
100	0.5021	0.2859	0.6859	24.9	29.7	0.342	15.38	−9.96
85	0.5075	0.2814	0.6906	25.1	29.9	0.310	15.06	−9.28
75	0.5113	0.2805	0.5929	25.1	29.9	0.304	15.04	−9.26
50	0.5214	0.2857	0.6861	25.0	29.7	0.341	15.03	−9.30
45	0.5235	0.2881	0.6837	24.9	29.6	0.358	15.02	−9.34
35	0.5278	0.2939	0.6776	24.8	29.3	0.399	14.71	−9.69
25	0.5323	0.3015	0.6698	24.6	29.0	0.454	14.40	−9.92
10	0.5393	0.3161	0.6549	24.2	28.4	0.558	13.68	−10.41

ln A_X = −2.6021 and ln A_W = 0.00469.

Table 3
Molecular sieve parameters and free energies for the dimer–tetramer equilibrium of oxyhemoglobin A in 0.25 M phosphate buffer, pH 7.4.

Conc (μg/ml)	ξ_i	σ_i	erfc σ_i	$\mathring{A}$	$\mathring{r}$	f_1	ln K	ΔG^0 (kcal/mole)
100	0.5232	0.2707	0.7018	25.3	30.4	0.234	13.97	−8.65
85	0.5188	0.2646	0.7089	25.5	30.6	0.190	15.28	−9.04
75	0.5184	0.2640	0.7088	25.5	30.6	0.186	15.67	−9.16
50	0.5259	0.2745	0.6978	25.2	30.1	0.261	15.59	−9.09
45	0.5289	0.2787	0.6884	25.0	30.0	0.291	15.48	−9.03
35	0.5364	0.2891	0.6826	24.9	29.6	0.365	15.23	−8.90
25	0.5458	0.3023	0.6690	24.6	29.0	0.459	14.99	−8.78
10	0.5636	0.3272	0.6436	23.9	27.9	0.637	14.92	−8.76

ln A_X = −1.8118 and ln A_W = 0.00818.

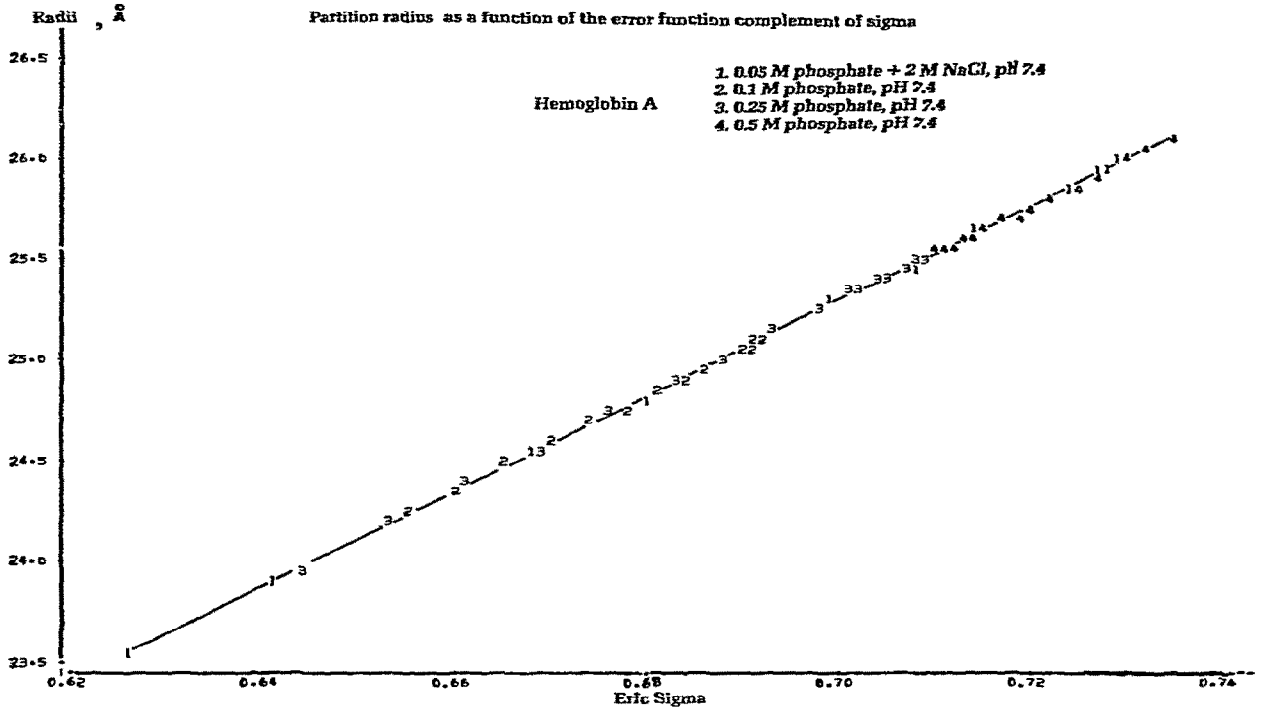
Radii, Å
Partition radius as a function of the error function complement of sigma
1. 0.05 M phosphate + 2 M NaCl, pH 7.4
2. 0.1 M phosphate, pH 7.4
3. 0.25 M phosphate, pH 7.4
4. 0.5 M phosphate, pH 7.4
Hemoglobin A
26.5
26.0
25.5
25.0
24.5
24.0
23.5
0.62
0.64
0.66
0.68
0.70
0.72
0.74
Erfc Sigma

Fig. 7.

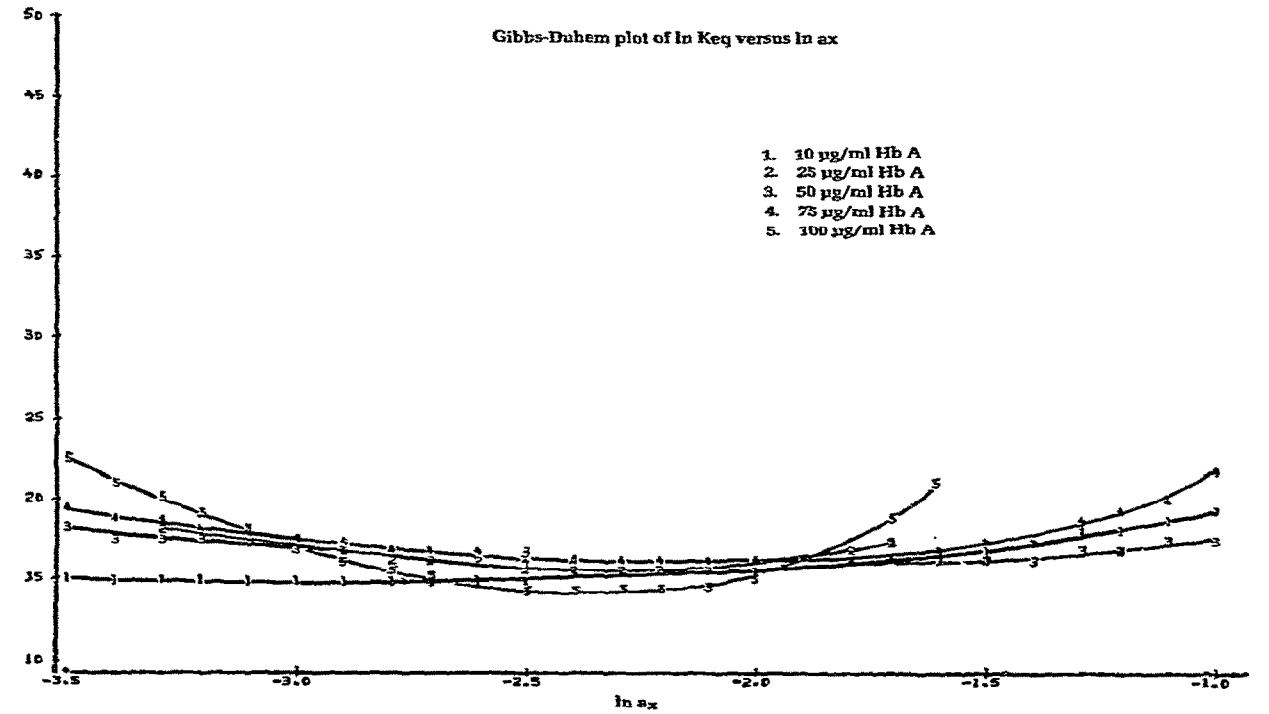
ln Keq
Gibbs-Duhem plot of ln Keq versus ln ax
1. 10 µg/ml Hb A
2. 25 µg/ml Hb A
3. 50 µg/ml Hb A
4. 75 µg/ml Hb A
5. 100 µg/ml Hb A
50
45
40
35
30
25
20
15
10
-3.5
-3.0
-2.5
-2.0
-1.5
-1.0
ln ax

Fig. 8.

Table 4
Molecular sieve parameters and free energies for the dimer–tetramer equilibrium of oxyhemoglobin A in 0.50 M phosphate buffer, pH 7.4.

Conc (μg/ml)	ξ_i	σ_i	erfc σ_i	$\mathring{A}$	$\mathring{r}$	f_1	ln K	ΔG^0 (kcal/mole)
100	0.4936	0.2390	0.7373	26.1	31.5	0.008	23.30	−13.78
85	0.4987	0.2469	0.7269	25.9	31.5	0.063	18.74	−11.11
75	0.5015	0.2512	0.7224	25.8	31.3	0.095	18.02	−10.68
50	0.5067	0.2590	0.7141	25.6	31.1	0.150	17.42	−10.32
45	0.5074	0.2601	0.7130	25.6	30.8	0.158	17.42	−10.32
35	0.5084	0.2170	0.7113	25.6	30.8	0 169	17.51	−10.44
25	0.5089	0.2625	0.7104	25.5	30.7	0.175	17.77	−10.53
10	0.5089	0.2625	0.7104	25.5	30.7	0.175	17.77	−10.53

$\ln A_X = -1.2711$ and $\ln A_W = 0.01154$.

Table 5
GLM linear parameters for $\bar{\sigma}_W = \Sigma_i \sigma_i f_i + \beta_1 C + \beta_2 C^2$ for a tetramer–dimer equilibrium as a function of hemoglobin concentration, in varying phosphate buffers, pH 7.4, at 25°C

	0.05 M PO_4^{-3}	0.1 M PO_4^{-3}	0.25 M PO_4^{-3}	0.5 M PO_4^{-3}
$\Sigma_i \sigma_i f_i$	0.3782	0.3579	0.3472	0.2617
β_1 (ml/mg)	−3.5910	−2.2665	−2.1421	+0.1223
β_2 (ml/mg)^2	+23.10	+18.47	+13.77	−3.48
Residue square	0.8277	0.9364	0.8325	0.8277
$PR > F$	0.1723	0.0635	0.1075	0.1723
STD deviation	0.0268	0.0054	00.0167	0.0189
Sum of square	2.79×10^{-3}	9.6×10^{-4}	2.8×10^{-3}	6.9×10^{-3}

The regenerated curve fits the experimental curve of the weight average partition coefficient as a function of concentration within a 90% confidence limit. β_1 and β_2 obtained from $(\bar{\sigma}_W/C) = (\Sigma_i \sigma_i f_i/C) + \beta_1 + \beta_2 C$ were consistent with values obtained from the expression $\bar{\sigma}_W = \sigma_1 f_1 + K f_1^2 \sigma_2 C_T + \beta_1 C_T + \beta_2 C_T^2$.

The values of $\Delta\bar{\nu}_{pref}$ are +6.45 at 100 μg/ml, +2.19 at 25 μg/ml and +1.49 at 10 μg/ml. Data at hemoglobin concentrations of 25 and 50 μg/ml do not fit a linear model within acceptable confidence limits, as determined from the residue square and an F-test. However, data at the other concentrations examined fell well within a 90% confidence limit. The values of $\Delta\bar{\nu}_x$ in the range of 0.05 M to 0.5 M phosphate, that is a range of $\ln A_X$ of −2.3476 to −1.2711, were approximately −4 to −56, suggesting that there is little or no binding of phosphate anions in the buffer system to either the dimer or the tetramer. On the contrary, these anions may take up more water molecules as the concentration of the phosphate buffer increases. It appears that a temperature-sensitive hydrated phosphate, perhaps $(H_2PO_4^-)nH_2O$, $(HPO_4^{-2})nH_2O$, or $(PO_4^{-3})nH_2O$, forms which further perturbs the equilibrium of this system.

Fig. 7. Partition radii as a function of the error function complement of sigma, grouping the data points of fig. 6 in linear form.

Fig. 8. Variation of ln *Keq* as a function of concentration of phosphate anion. Activity coefficients of various phosphates were obtained from fig. 1. The equilibria of the various hemoglobin concentrations were determined from the weight fractions of monomer given in tables 1–4.

Table 6
The effect of phosphate anions (0.05 M to 0.5 M NaH_2PO_4 buffer, pH 7.4 at 25°C) on the preferential binding ($\Delta\bar{\nu}$ pref) and solvation parameters ($\Delta\bar{\nu}_X$ and $\Delta\bar{\nu}_W$) of the tetramer–dimer equilibrium as a function of concentration of oxyhemoglobin

	Concentration (μg/ml)				
	100	75	50	25	10
$\frac{d \ln K}{d \ln A_X} = \Delta\bar{\nu}_{pref}$	+6.45	–	–	+2.19	+1.49
$\Delta\bar{\nu}_X$	−56.0	−12.9	−4.0	–	−3.7
$\Delta\bar{\nu}_W$	+13,452	+2835	+984	–	+1124
1. Residue square	0.9893	0.9863	0.4042	0.4526	0.6258
2. $PR > F$	0.1035	0.1171	0.7719	0.3272	0.2089
3. Standard deviation	1.357	0.235	0.981	2.432	1.163
4. Sum of square of error	1.844	0.055	0.964	11.833	2.706

$\ln K$ versus $\ln A_X$ shown in fig. 8 are used to calculate $\Delta\bar{\nu}_X$ and $\Delta\bar{\nu}_W$. $\ln A_X$ values are extracted from Robinson and Stokes [27], then compared with the activity coefficients of NaH_2PO_4 as a function of molal concentration at 25°C. (CRC Handbook of Chemistry and Physics, 50th Ed. D-121, 1969). The Gibbs-Duhem expression is obtained by combining two osmotic coefficients: $\phi = -(55.56/\nu m_X) \ln A_W$; $\phi = +(1000/\nu W_X m_X) \ln A_X$, where W_X is the molecular weight of the Hofmeister salt. Thus, salt activity, A_X, may be determined by integration of the Debye-Hückel-Onsager equation, an expression used for evaluation of the electrostatic free energy contribution. The value of $\Delta\bar{\nu}_{pref}$ is determined by the change in the equilibrium constants between the phosphate anions and the tetramer–dimer equilibrium of oxyhemoglobin. It is evaluated based on eq. (11), fitting $\ln A_X$ and $\ln A_W$ to $\ln Keq$, where $\ln Keq$ is a function of $\ln A_X$ at a given temperature.

Fig. 9 shows a plot of the standard free energy change of association from dimer to tetramer, expressed in terms of kcal/mole tetramer formed. The curves show the influence of the phosphate anion on the free energy change as a function of hemoglobin concentration.

At high phosphate concentrations the activity of the salt at $\ln A_X = -1.5000$ seems to have a greater

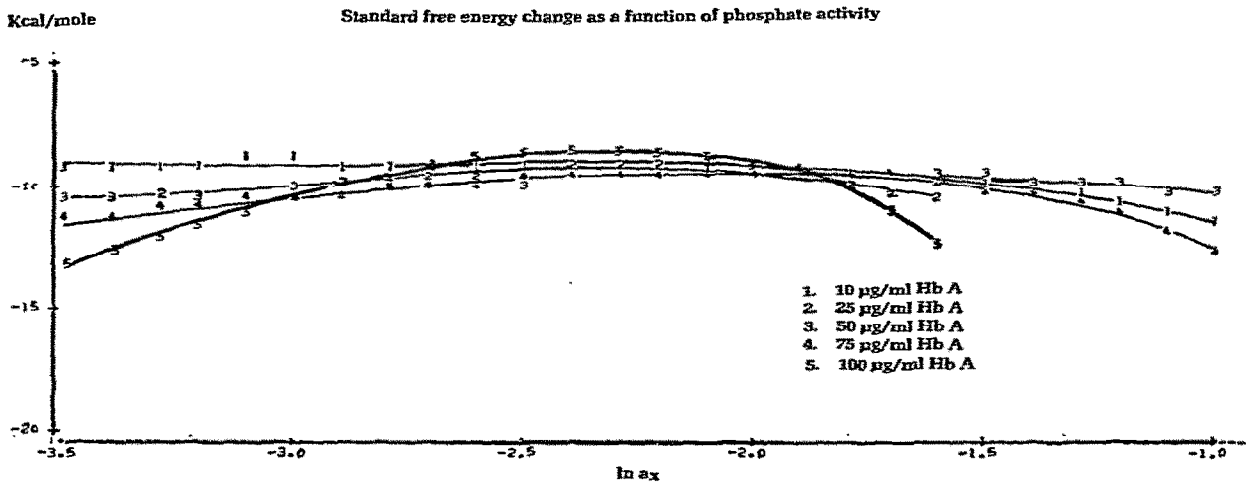

Fig. 9. Dependence of the Gibbs free energy change as a function of $\ln A_X$. The activity coefficients of various phosphates were obtained from fig. 1.

influence on tetramer formation than at $\ln A_x =$ -3.0000. The standard free energy change at $\ln A_x =$ -3.2476 is 9.4 ± 0.2 kcal/mole as compared with a value of 8.9 ± 0.7 kcal/mole in 0.1 M Tris/HCl, 1 mM Na_2EDTA, 0.1 M NaCl, reported by Ip and Ackers [10]. ΔG^0 in $\ln A_x = -1.2711$ is 10.96 ± 0.05 kcal/mole indicating that approximately 11 kcal are required to dissociate one mole of tetramer into dimer. At 100 μg/ml, fig. 9 indicates that approximately $13 \sim 14$ kcal are required to dissociate the hemoglobin tetramer into dimer, clearly establishing that the dissociation is dependent on both the concentrations of hemoglobin and phosphate in the system.

4. Discussion

Our examination of the dimer–tetramer equilibrium of oxyhemoglobin by scanning molecular sieve chromatography reveals that the correlation of the partition coefficient with the partition radii, although widely reported in the past, is not a representation of the absolute magnitude of the particle radius [33]. Use of eq. (14) enables us to record the partition radii as a function of concentration, permitting us to observe the changes in the equilibrium state as the components undergo chemical reaction. The difference profile method, therefore, promises to have wide applicability to further studies on preferential binding and solution phenomena in various self-associating protein systems, primarily because of the increased accuracy in determining the $(dt/d\bar{x})$ parameter.

Based on eq. (14), it is possible to determine the variation of the Stokes radii of the spheroid hemoglobin molecules undergoing tetramer–dimer dissociation within 5 Å. The Stokes radii varied from 27 to 32 Å in this dissociating system, in good agreement with reported values of 31–32 Å for the hemoglobin tetramer [34,35].

Klotz [36] and Tanford [37] have shown that a Hofmeister series of anions can modify the association (or dissociation) equilibria [38–41] of protein either by preferential binding to one of the equilibrating species or by changing the activities of added salt or water. Increasing the phosphate concentration from 0.05 to 0.5 M increases the degree of dissociation, a change reflecting an increase in hydrophobic interaction since the phosphate anions will "salt out" non-polar groups [23]. It has been shown that Hofmeister specificity depends on the interaction between the anions and such non-polar groups. The dimer–tetramer equilibria of oxyhemoglobin proves an excellent model for evaluating the effect of neutral salts, since the self-association process involves both inter-subunit contact between hydrophobic side chains and concomitant changes in hydrogen bonding and salt bridges.

Our results suggest that the mode of action of the phosphate anions in a hemoglobin solution is not what would be predicted by other studies. They appear to form hydrated phosphates which enhance the formation of tetramer by perturbing the solvation layer of the hemoglobin dimer. Because of the difficulty in determining the true values of $\Delta\bar{\nu}_w$ and $\Delta\bar{\nu}_x$, however, the specific mode of action of this electrolyte at the binding site can only be suggested by our results. Certainly any further studies should define $\Delta\bar{\nu}_x$, $\Delta\bar{\nu}_{H^+}$ and $\Delta\bar{\nu}_{H_2O}$ as a function of temperature for the phosphate anion as well as the full Hofmeister series.

References

[1] E.E. Brumbaugh and G.K. Ackers, J.Biol. Chem. 244 (1968) 6315.
[2] E.E. Brumbaugh and G.K. Ackers, Anal. Biochem. 41 (1971) 543.
[3] E.E. Brumbaugh, E.E. Saffen Jr. and P.W. Chun, Biophys. Chem. 19 (1979) 000.
[4] E.E. Saffen Jr., E.E. Brumbaugh and P.W. Chun, Fed. Proc. (1978).
[5] G.K. Ackers and T.E. Thompson, Proc. Nat. Acad. Sci. U.S. 53 (1965) 342.
[6] E. Chiancone, L.M. Gilbert, G.A. Gilbert and G.L. Kellett, J. Biol. Chem. 243 (1968) 1212.
[7] G.K. Ackers, in: The proteins, Vol. 1, ed. H. Neurath and H.L. Hill (Acad. Press, New York, 1975) 3rd Edition.
[8] G.K. Ackers and H.R. Halvorson, Proc. Nat. Acad. Sci. U.S. 71 (1974) 4312.
[9] G.K. Ackers, M.J. Johnson, F.C. Mills and S.H.C. Ip, Biophys. Biochem. Res. Comm. 69 (1976) 135.
[10] S.H.C. Ip and C.K. Ackers, J. Biol. Chem. 252 (1977) 82.
[11] R. Valdes Jr. and G.K. Ackers, J. Biol. Chem. 252 (1977) 74.
[12] R. Valdes Jr. and G.K. Ackers, J. Biol. Chem. 252 (1977) 88.
[13] A.D. Barksdale and A. Rosenberg, J. Biol. Chem. 253 (1978) 4881.

[14] J.O. Thomas and S.J. Edelstein, Biochemistry 10 (1971) 477.
[15] J.O. Thomas and S.J. Edelstein, J. Biol. Chem. 248 (1973) 2901.
[16] G.L. Kellett, J. Mol. Biol. 59 (1971) 401.
[17] D. Elbaum and T.T. Herskovits, Biochemistry 13 (1974) 1268.
[18] R. Benesch, G. Macduff and R.E. Benesch, Anal. Biochem. 11 (1965) 81.
[19] M.F. Perutz, Nature 228 (1970) 726.
[20] W.J. Evans, L. Forlani, M. Brunori, J. Wyman and E. Antonini, Biochem. Biophys. Acta 214 (1970) 64.
[21] J.D. Sakura and F.J. Reithel, in: Methods in enzy:, XXVI, part C, eds. C.H.W. Hirs and S.N. Timasheff (Acad. Press, N.Y., 1972).
[22] M. Tainsky and S.J. Edelstein, J. Mol. Biol. 75 (1973) 735.
[23] P.H. Von Hippel and T. Schleich, in: Structure and stability of biological macromolecules, eds. S.N. Timasheff and G.D. Fasman (Marcel Dekker, New York, 1969) p. 417.
[24] R.C. Williams Jr. and K.Y. Tsay, Anal. Biochem. 54 (1973) 137.
[25] P.W. Chun, E.E. Saffen Jr. and J.O. Oeswein, Biophysical Chem., submitted.
[26] P.W. Chun and E.E. Saffen Jr., Biophysical Chemistry, submitted.
[27] R.A. Robinson and R.H. Stokes, in: Electrolytic solutions (Butterworths, London,.1959).
[28] CRC Handbook of Chemistry and Physics, eds. R.C. Weast and Ture (The Chemical Rubber Co., 1969).
[29] G.K. Ackers, J. Biol. Chem. 242 (1967) 3237; 243 (1968) 2956.
[30] G.K. Ackers, in: Advances in protein chemistry, Vol. 23, (Academic Press, New York, 1970) p. 343.
[31] G.K. Ackers, M.L. Johnson, F.C. Mills, H.R. Halvorson and S. Shapiro, Biochemistry 14 (1975) 5128.
[32] A.J. Barr, J.H. Goodnight, J.P. Sall and J.T. Helwig, A user's guide to SAS, 76, Statistical analysis system, University of Florida, Circa Computing Facilities, 1976.
[33] H.S. Warshaw and G.K. Ackers, Anal. Biochem. 42 (1971) 405.
[34] G. Kegeles and G.J. Gutter, J. Am. Chem. Soc. 73 (1951) 3770.
[35] R.L. Baldwin, P.J. Dunlop and L.J. Gasting, J. Am. Chem. Soc. 77 (1955) 5235.
[36] I.M. Klotz, Arch. Biochem. Biophys. 116 (1966) 92.
[37] C. Tanford, J. Mol. Biol. 39 (1969) 539.
[38] H. Edelhoch and J.C. Osborne, Adv. Prot. Chem. 30 (1976) 183.
[39] K.C. Aune, L.C. Goldsmith and S.N. Timasheff, Biochemistry 10 (1971) 1617.
[40] S. Formisano, M.L. Johnson and H. Edelhoch, Proc. Nat. Acad. Sci. U.S. 74 (1977) 3340.
[41] S. Formisano, M.L. Johnson and H. Edelhoch, Biochemistry 17 (1978) 1468.